Reports

X-Ray Spectra from Three Cosmic Sources

Abstract. *Three cosmic x-ray sources have been observed from a water-launched rocket carrying two x-ray detectors to an altitude of 200 kilometers. The x-ray spectra, measured in the photon energy range between 1 and 40 kiloelectron volts, are all different. The sources in order of hardness of spectra are Cyg XR-1, Tau XR-1, and Sco XR-1. The intensity of Sco XR-1 decreased at low photon energies. The differences in spectra might be interpreted as evidence of different source mechanisms.*

Cosmic x-ray sources other than the sun were first detected in 1962 (*1*). Since then one source, Taurus XR-1, has been precisely located with a lunar occultation experiment (*2*) and identified as the Crab Nebula. Nine other sources have been discovered and located (*3, 4*) to accuracy of the order of 1°. The x-ray spectrum from the strongest of these sources, Scorpius XR-1, has been measured (*5*) in the photon energy range between 2 and 20 kev.

In our experiment, detectors covering a larger energy range were used. The strong Scorpius source was observed again, and spectral data were gathered for x-rays from the Crab Nebula and Cygnus XR-1.

No precise measurement of source location was attempted because the orientation of the rocket axis was known only to 1 or 2 degrees, and the collimation was deliberately made rather broad to ensure good statistical accuracy. The positions of the sources that are given by Bowyer *et al.* (*3*) and by Fisher *et al.* (*4*) were used to determine the optimum launch time.

Two detectors were used: a thin-window proportional counter and a phoswich (phosphor-sandwich) scintillation detector. These detectors were carried by a two-stage Hydra-Iris rocket system which was fired from a floating launcher. The rocket was launched on the morning of 28 October 1965 from a point in the open sea about 720 km southwest of southern California. The payload, which was 30 cm in diameter, coasted out of the atmosphere still attached to the burned-out Iris sustainer. Apogee of the flight occurred at 126°38′W, 29°44′N, and 200 km altitude, at $18^h05^m17^s$ U.T. The payload was spin-stabilized at about 2.5 rev/sec. The precession angle was observed to be less than 1°, which makes precession negligible in the analysis of this experiment. The vehicle was tilted about 10° west-southwest of the vertical during the flight. The rocket spin axis pointed at a spot on the celestial sphere at right ascension 11.3^h and declination 28.0°.

The orientation of the detectors was perpendicular to the rocket axis. Collimation was rather broad in the vertical direction and narrow in azimuth. Thus, since the rocket axis was approximately vertical during the flight, the detectors viewed sources located in a wide band just above the horizon. As the rocket spun, the detectors viewed in rapid succession objects at different azimuth. The experiment was planned to observe the strong source in Scorpius (Sco XR-1) and the two weaker sources Tau XR-1 and Cyg XR-1. The cluster, toward the galactic center, of sources which were unresolvable with these detectors was planned to be below the horizon. A solar sensor was used to determine rocket orientation and to measure the azimuthal detector angle-of-view during the flight. A three-axis gyro system also measured the rocket motion during flight.

Both detectors were turned on just before launch. Calibration sources were mounted on the inside of the nose cone, and, during the first 90 seconds of flight, the detector response to these sources was monitored. At an altitude of 90 km the nose cone was jettisoned, carrying the calibration sources with it. Data were taken for the next 300 seconds by the proportional counter. The phoswich detector suffered from high-voltage breakdown during part of the flight. For about 240 seconds (of time) there were no breakdown difficulties, and our data were gathered in this interval.

The proportional counter consisted of a main counter surrounded on three sides by guard counters set to reject cosmic rays. All counters were filled from a common gas supply with 1.3 bar (absolute) of 90 percent argon and 10 percent CH_4 (P-10) gas just before launch. The center counter window was 0.15-mil Mylar coated with 1000 Å of aluminum and supported on an egg-crate style collimator of 91 cm^2 open area. The extinction angles of the collimator were ± 7° perpendicular to the counter axis and ± 30° parallel to the axis.

Signals from the center counter amplifier were fed to a discriminator scaler and also to a gate circuit followed by a pulse stretcher. The output of the stretcher was telemetered to the ground and was also fed back to close the gate while the pulse was being stretched. The gate could also be closed by a discriminator triggered by the guard counters to reduce the background from cosmic rays.

Although the stretcher was limited to a maximum rate of about 500 count/sec, the shape of the output spectrum was essentially independent of count rate. The discriminator fed by the center counter was set at 4.1 kev so that a direct count-rate correction could be made to the stretcher count by comparing the scaler count with all stretcher counts above 4.1 kev.

Some distortion at high count rate was noted in preflight tests. For the rates encountered during the flight the corrections for shifts in the count rate were less than 10 percent in all cases.

The detector efficiency, calculated from published values of the absorption coefficients of Mylar and argon, is shown in Fig. 1. The points indicated are postflight measurements of the transmission of 0.15-mil Mylar coated with 1000 Å of aluminum. Also shown in the figure is the measured resolution at 5.9 kev.

The phoswich detector was a piece of cesium iodide (11.4 by 3.8 by 0.3 cm) completely surrounded by plastic scintillator, the thickness of which was 0.10 cm in the front and 0.64 cm in the back and sides. This composite scintillator was viewed by three Ascop 541-A photomultiplier tubes 2.54 cm in diameter. Output pulses from these tubes were added, amplified, and passed through a rejection gate. If the scintillator light pulse contained a fast component (caused by a charged particle depositing energy in the plastic scintillator), the gate was closed and the pulse rejected. The pulses that were not rejected (events which deposited energy only in the cesium iodide) were stretched to a length of 1.5 msec and telemetered directly to the ground. Pulse height was conserved in this process and pulse-height analysis was done on the ground with the telemetered data.

The scintillator was collimated to a half transmission angle of $\pm 10°$ in azimuth and $\pm 35°$ in angle of elevation by a silver collimator. The entire collimator and detector assembly was shielded on the back and sides by lead. Thus the detector was sensitive only to photons coming from the area viewed through the collimator. Pulses caused by charged particles passing through the plastic scintillator were rejected. The detector, however, was not capable of rejecting events arising from photons created by cosmic rays in the collimator or photomultipliers when these cosmic rays did not pass through the plastic scintillator. Mylar (0.0025 cm thick) was placed over the front of the collimator to prevent low-energy electrons from striking the collimator and generating bremsstrahlung there.

Fig. 1 (left below). Proportional counter efficiency as a function of photon energy. The solid curve is the calculated counter efficiency. Experimentally measured points are shown as dots. The dashed curve is the measured counter response to 5.9-kev x-rays. FWHM, full width at half maximum. Fig. 2 (right below). Phoswich detector efficiency as a function of photon energy. The solid curve is the calculated phoswich efficiency. Dots are experimental measurements with fluorescent x-rays. The 6-kev experimental point is low because of counter resolution and a low-energy electronic cutoff. The dashed curve is the measured phoswich response to 22-kev x-rays.

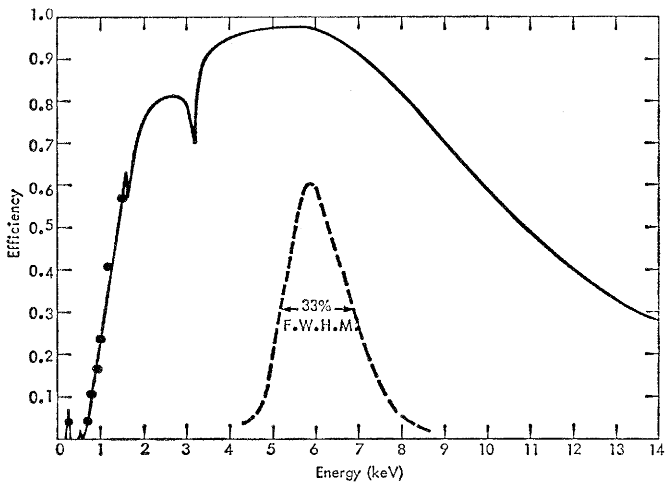

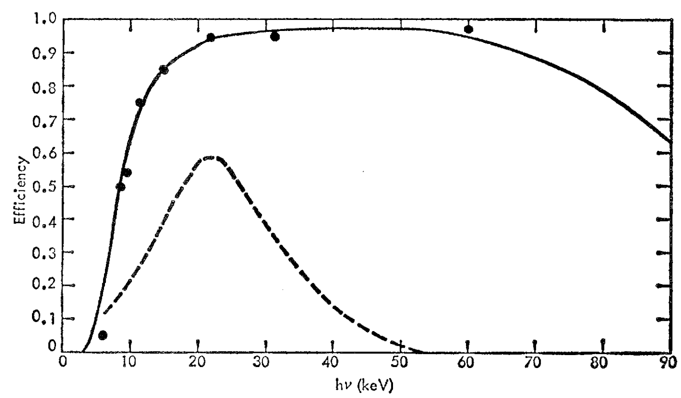

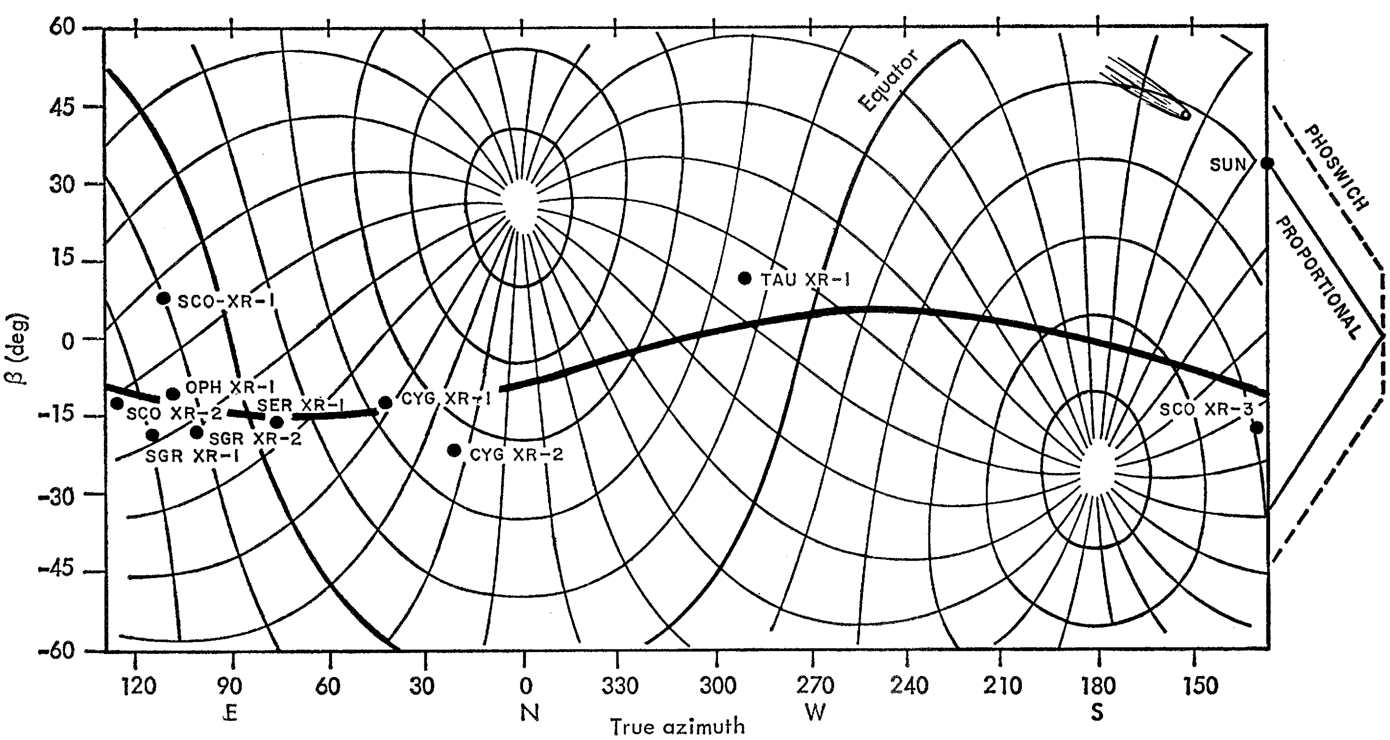

Fig. 3. The celestial sphere as viewed by the detectors. The angle β is the detector-view angle measured from a line perpendicular to the detector face in the plane determined by this line and the rocket axis. Contours of constant right ascension and declination have been drawn every 15°. The comet Ikeya-Seki was just outside the field of view of the detectors.

The detector efficiency as a function of photon energy is illustrated in Fig. 2. To reach the cesium iodide, photons had to pass through 0.0025 cm of Mylar, 0.0025 cm of aluminum, and 0.10 cm of plastic scintillator. The low-energy cutoff at about 5 kev is caused by this material. The decrease of efficiency at the higher energy is caused by both the thinness of the cesium iodide and the fact that the rejection circuit rejected very large pulses even if they contained no fast time component. Figure 2 also shows the measured resolution for 22-kev photons. Resolution was sacrificed to get a large area of scintillator. Maximum effective detector area was measured as about 36 cm^2. Before flight the detector response to photons ranging in energy from 8 to 88 kev was measured with sources and fluorescent x-rays from an x-ray machine. These measured resolution functions were used to interpret the flight data.

Figure 3 shows a computer-generated plot of the celestial sphere as viewed by the detectors. The poles of this projection, which are off the scale of the figure, correspond to the intersections of the rocket longitudinal axis with the celestial sphere. Thus, β equal to 0° is the detector center line and the vertical collimation of both detectors is indicated. The x-ray horizon (solid line) has been drawn 5° below the sea level horizon. This x-ray horizon is determined by the zenith coordinates of the rocket at apogee and corresponds to approximately 10^{-4} g/cm^2 of atmosphere between source and detector (an attenuation of about 50 percent for 1-kev photons). The sources and source positions indicated in Fig. 3 are those given by Bowyer *et al.* (*3*).

Figure 4 shows the total number of counts in the two detectors plotted as a function of azimuth. Figure 4 may be compared directly with Fig. 3. Four sources are visible in Fig. 4; in order of prominence they are: Sco XR-1, Sun, Tau XR-1, and Cyg XR-1. To illustrate the spectral differences between sources, data have been plotted for each detector at two bias settings. All counts observed in the proportional counter are compared to all counts above 1.7 kev, and all counts observed in the phoswich detector (threshold approximately 5 kev) are compared with all phoswich counts greater than about 30 kev. Few photons from the sun were observed with energies greater than 1.7 kev. The Scorpius source is most prominent in both detectors at the lower energies but is not visible at energies greater than 30 kev. The Crab Nebula and Cyg XR-1 are equally prominent in the phoswich data, but there is a striking difference between these two sources as seen by the proportional counter. There is a hint of Ser XR-1 in the proportional counter data but this is not prominent enough to be a usable observation. The data are not corrected for count rate.

The data of Fig. 4 were generated by running the tape-recorded rocket telemetry signal through an electronic processing system. The solar sensor pulse was used to start a ramp which was sampled each time a detector pulse occurred. The pulses were fed to a pulse-height analyzer which produced a plot of number of counts as a function of azimuthal position. The data of Fig. 4 represent four runs of the telemetry tape through this system. Spectra were then obtained by gating the analyzer in given azimuth intervals and doing conventional pulse-height analysis.

Figure 5 shows the observed x-ray intensity from Sco XR-1 versus photon energy and the previously measured x-ray intensity from this source. Pulse-height spectra were obtained from counts in the peak centered at 115°. Background data taken from the regions around 60° and 240° were subtracted. The pulse-height spectra were then corrected for counter efficiency and dead time. The dead-time correc-

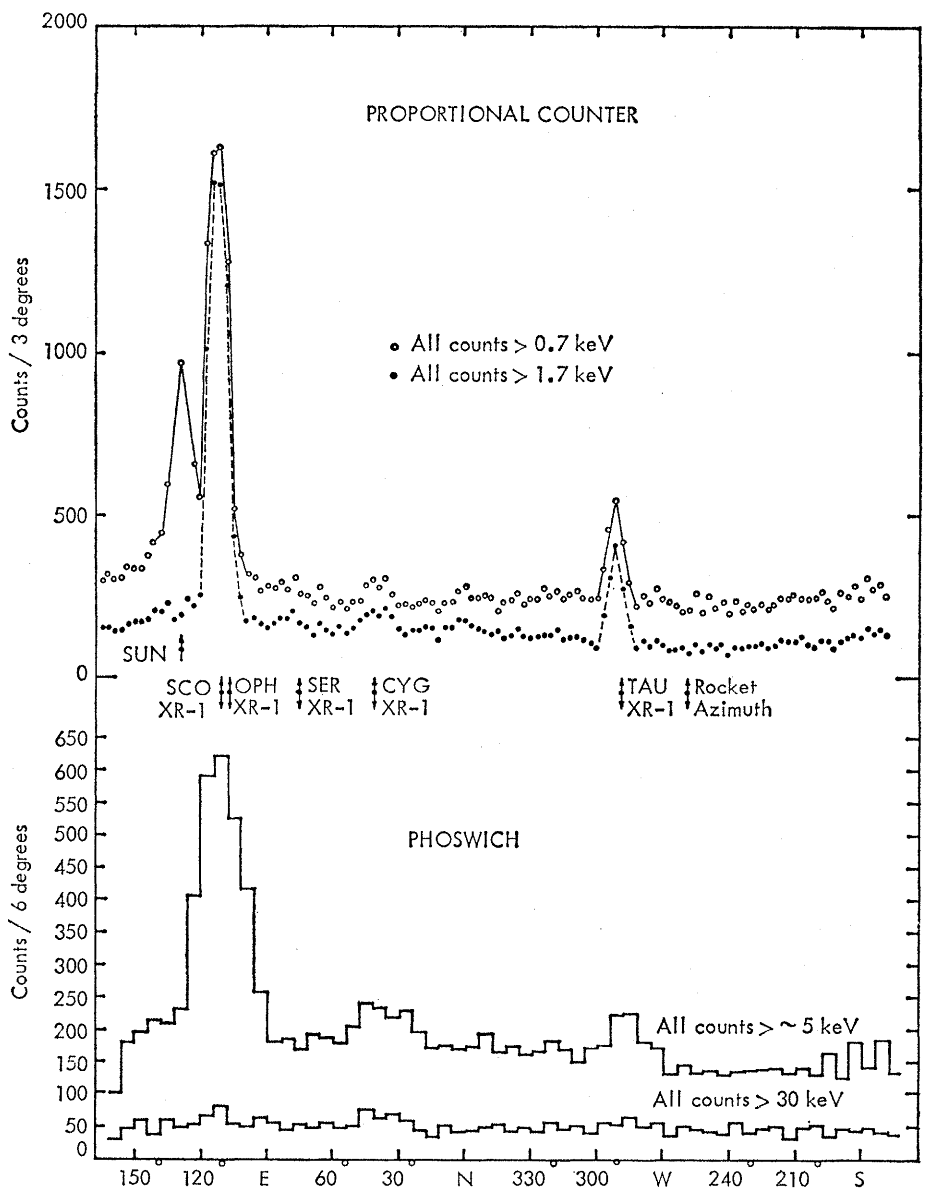

Fig. 4. Number of counts observed in the proportional counter and in the phoswich detector as a function of azimuth. Integral counting rates are given for each detector at two bias levels.

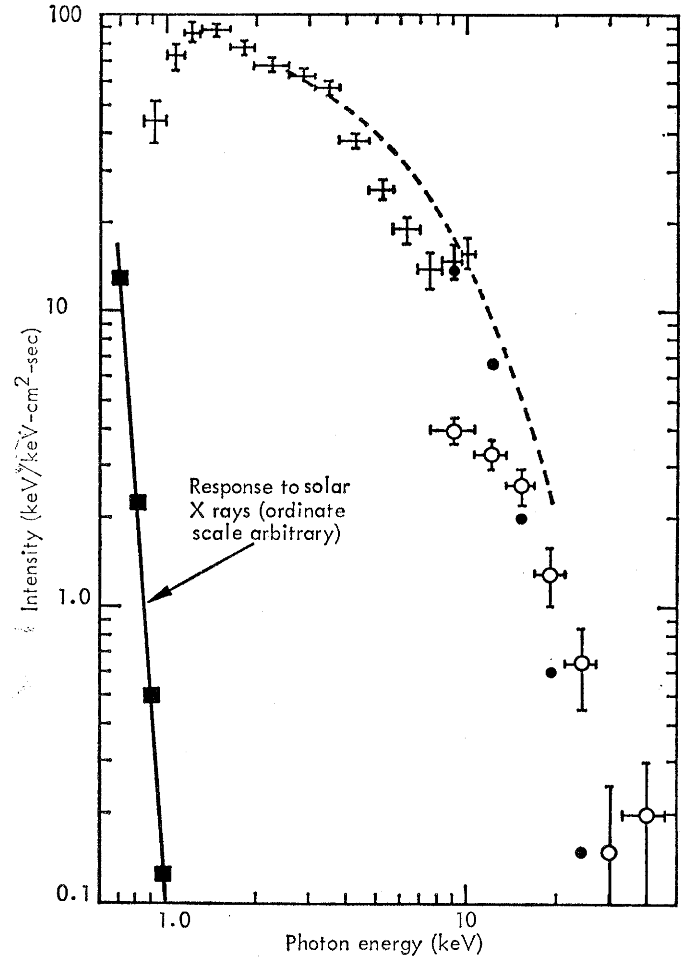

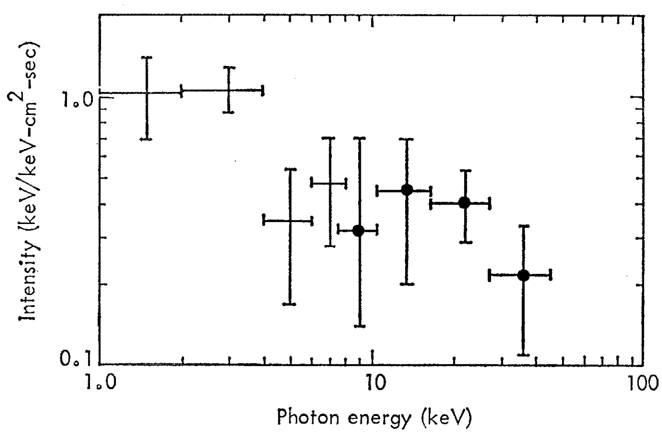

Fig. 5 (left). Intensity of Scorpius XR-1 as a function of photon energy. Proportional counter data are shown by crosses. The data from the phoswich detector, uncorrected for resolution or efficiency, are shown by open circles. The closed circles are the phoswich data corrected for counter efficiency and resolution on the assumption of a smoothly decreasing spectrum. The intensity spectrum from Sun, corrected for proportional counter efficiency, is also given so that the shape of the low-energy region of both spectra may be compared. Dashed line shows spectrum on 12 June 1965 (*5*). Fig. 6 (below left). Intensity of Taurus XR-1 (Crab Nebula) as a function of photon energy. Data points are the spectrum taken with the proportional counter and phoswich detector and corrected as described for Fig. 5. The dashed line is the measurement of Peterson *et al.* (*6*). Fig. 7 (above). Intensity of Cygnus XR-1 as a function of photon energy. Data points are those taken with proportional counter and phoswich detector and corrected as described for Fig. 5. Error bars are mostly a result of background subtraction. The energy intervals between data points have been increased to improve statistics. Fig. 8 (below). Two theoretical fits to the intensity of Sco XR-1 plotted against photon energy. Data points are from Fig. 5. The dashed line is the spectrum of a black body with a characteristic temperature of 0.8 kev (9×10^{6}°K). The solid line is a spectrum of the form $I\,(h\nu) \propto e^{-h\nu/kt}$ with $kt = 4$ kev ($T = 4.6 \times 10^{7}$°K). The dot-dash curve shows the effect of transmission of this spectrum through 10^{-2} g/cm^2 of hydrogen.

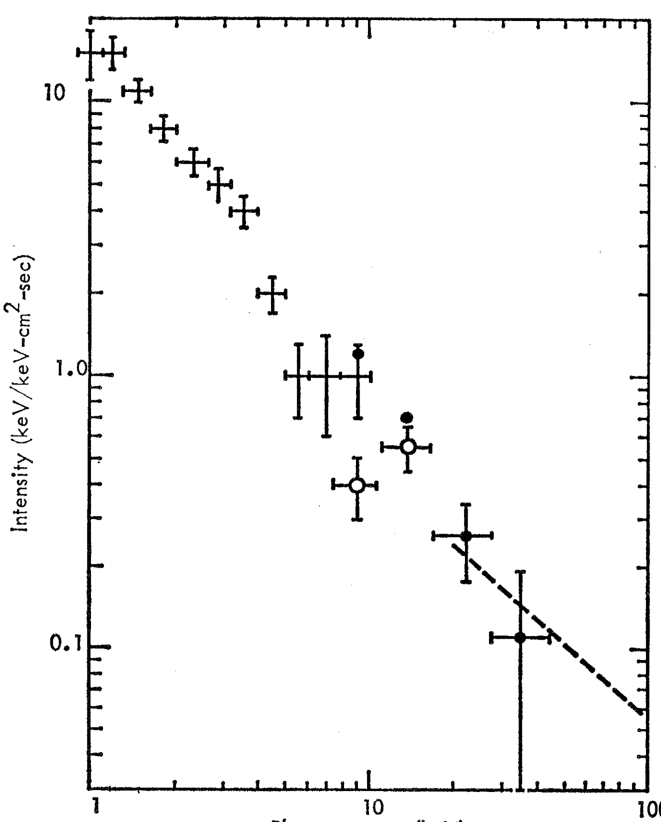

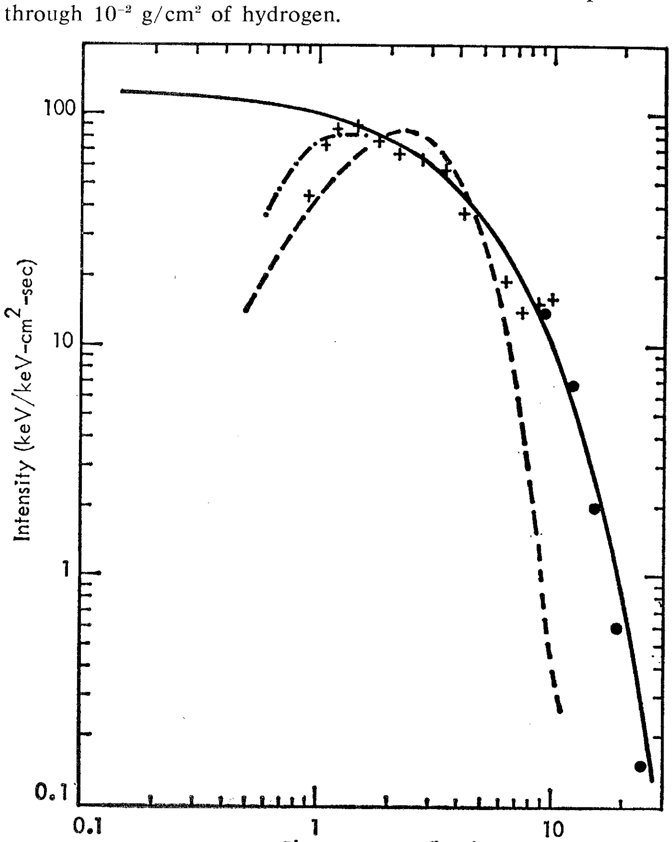

tion for the phoswich detector was about 15 percent. The count-rate correction factor for the proportional counter was 7.3, obtained directly from the ratio of scaler count to stretcher count above 4.1 kev. All preflight checks indicated that the shape of the spectrum was not appreciably distorted by count-rate changes.

The open circles in Fig. 5 show phoswich data uncorrected for counter efficiency and resolution. Because of the steepness of the spectrum and the poor resolution of this detector, this correction is large. For example, 20-kev photons produce an appreciable fraction of pulses with heights corresponding to those from 40-kev photons. Since the resolution of this detector was measured at many photon energies before flight, it is possible to correct the observed pulse-height spectrum to obtain the true photon spectrum. This is true only if the spectrum is smoothly varying; there is every indication that this Scorpius spectrum is smoothly varying. The spectral form given by Chodil *et al.* (*5*) was used to correct the open circles of Fig. 5 into an intensity spectrum as indicated by closed circles. Error bars on data from both detectors indicate counting statistics.

Figure 6 shows the intensity of x-ray energy from the Crab Nebula as a function of photon energy. Spectral data were obtained from counts falling in the peak centered on 290°; the background subtracted was taken from the region centered around 240°. The proportional counter data have been corrected for counter efficiency. Error bars indicate counting-statistics. The count-rate correction factor determined from the scaler data for the proportional counter was 2.3. The dead-time correction for the phoswich was negligible. Once more the open circles are the phoswich data uncorrected for counter efficiency and resolution. Error bars on the phoswich points indicate counting statistics, which are now appreciable because the source is considerably weaker than Sco XR-1. The phoswich data, corrected for resolution and counter efficiency, are again indicated by closed circles. This correction is smaller here because the spectrum does not fall off as steeply as that of Sco XR-1.

The dashed line in Fig. 6 is that measured by the balloon experiment of Peterson on 23 September 1965 (*6*).

Figure 7 shows the intensity of Cyg XR-1 versus photon energy. Error bars indicate counting statistics. The spectral data were obtained from the peak centered at 40 degrees. Background data were obtained from the regions centered at 0°, 60°, and 240°. Uncertainties in background are large, and the spectrum appears to be hard enough so that corrections to the phoswich data for resolution are negligible compared to other uncertainties. The proportional counter data have been corrected for counter efficiency and atmospheric attenuation, since this source was 2° below the sea-level horizon at apogee.

The shape and intensity of the measured Scorpius (Sco XR-1) spectrum agree reasonably with the measurement on 12 June (*5*). The spectral shape between 2 and 10 kev appears slightly different however, and the intensity at photon energies greater than 20 kev appears somewhat lower in this measurement. The experimental difficulties are such that we cannot say whether these differences are real. These uncertainties arise from two factors. (i) The proportional counter data were taken at a high counting rate. A large dead-time correction was necessary at these rates and preflight data taken with calibration sources indicated that there were small spectral distortions at high counting rates. (ii) Since the Scorpius spectrum falls off steeply above 10 kev, the correction to the phoswich data for counter resolution is large. Because of these large corrections to both sets of data the differences between the June and October data are not definitely significant. The measured flux between 10 and 20 kev is, however, about a factor of 10 higher than that measured by Giacconi *et al.* in October 1964 (*7*).

The most interesting feature of this measured spectrum is the fall-off in intensity observed at photon energies less than 1.5 kev. It is difficult to prove that this is not an instrumental effect. In this region the correction for window transmission is large, the counter resolution is broad, and counting rates for the Sco XR-1 source were high.

Window transmission has been measured at our laboratory with the use of fluorescent x-rays, a proportional counter, and a Mylar-aluminum window identical to that used in the flight. The measurements agree with the transmission calculated with carbon and aluminum absorption coefficients (Fig. 1).

The counter response to solar x-rays is given in Fig. 5 for comparison. In the region below 800 ev, window transmission was $\leqq 10$ percent, and the response of the electronics of the detector was not linear. Thus, these data cannot be reliably given as the intensity of solar x-ray emission. They do illustrate that the system was operating about as expected in this region. Relatively few low-level pulses were seen in the Scorpius spectrum. It seems clear that the x-ray intensity from Sco XR-1 does not rise steeply at low energies. A straightforward analysis of the data indicates the fall-off shown in Fig. 5. Although preflight calibrations made at both higher and lower counting rates than the rate from the Scorpius source gave no indication of serious distortion, the 5.9-kev energy of the source used did not provide a conclusive test of the system response in the 1-kev region.

Atmospheric thickness between source and detector was calculated to be less than 5×10^{-5} g/cm^2 (130 km altitude) during the time data were taken. Transmission of 800-ev photons through this amount of atmosphere is calculated to be 75 percent. Therefore, the fall-off, if real, results either from a property of the source or from absorption by interstellar material.

Figure 8 illustrates a black-body spectrum fitted to the Scorpius spectrum of Fig. 5. The characteristic black-body temperature is 0.8 kev. The fit is reasonable except at photon energies greater than about 7 kev. Some additional source mechanism must be invoked to explain the observed high-energy photons. Cameron (*8*) has postulated that a neutron star with high-energy electrons in the surrounding magnetosphere could produce such a black-body spectrum with a high-energy tail.

Figure 8 also shows a spectrum of the form $I(h\nu) \propto e^{-h\nu/kt}$ with $kt = 4.0$ kev, where I is intensity, $h\nu$ is the energy of the photon, and kt is the temperature in kilovolts. Data from the June flight were best fitted with a spectrum of this form with $kt = 5.0$ kev. This spectral form is that expected from a thin, hot plasma source. To give a feeling for the influence of interstellar absorption, Fig. 8 also shows this spectrum after transmission through 10^{-2} g/cm^2 of neutral hydrogen. If one assumes an interstellar density (*9*) of 1 hydrogen atom per cubic centimeter, this thickness corresponds to a distance of about 2 parsec, which is about twice the distance from the sun to the Crab Nebula. Since it is thought that other weaker sources observed are clustered around the galactic center (*3*), which lies at a distance of about 8 parsec, the Scorpius source would then be an object of comparable absolute intensity.

The measured spectrum from the Crab Nebula agrees with that of Peterson *et al.* (*6*) for photon energies greater than 20 kev. The shape of this spectrum is different from that of Sco XR-1. Our data are reasonably fitted by a straight line drawn on Fig. 6. Thus, the spectral intensity is of the form $I(h\nu) \propto (h\nu)^{-1.3\pm0.2}$ between 1 and 20 kev. Peterson finds that, between 20 and 100 kev, $I(h\nu) \propto (h\nu)^{-0.9\pm0.1}$. X-rays from the Crab Nebula are expected to be synchrotron radiation because optical and radio emission of this form has been observed. This is the expected spectral shape for such synchrotron radiation if the differential spectrum (*10*) of the high-energy electrons producing x-rays is of the form $N(E) \propto E^{-m}$, where $N(E)$ is the number of electrons of energy E, and m is a constant. For the data of Fig. 6, $m \approx 3.5$. Our counting errors were too large to allow reliable spectral information below 1 kev of x-ray energy.

Because of the apparent weakness of the Cygnus source there are large uncertainties in the measured spectral data caused by statistics and background subtraction. It is clear, however, that the x-radiation from this source is harder than that from the others. The Cygnus source was close to the horizon when this measurement was made.

From the position given by Bowyer *et al.* (Fig. 3), calculated atmospheric thickness between source and detector at apogee is approximately 10^{-4} g/cm^2, and atmospheric absorption should be negligible down to 1.5-kev energy. The source position would have to be in error by about 6° for atmospheric attenuation to account for the observed spectral hardness. The source intensity is much weaker than that given by Bowyer *et al.* who measured Cyg XR-1 in the region of 1.5- to 4-kev photon energy to be 1.3 times as strong as Tau XR-1. If the source position is correct, this source has changed considerably since the time of the measurement (June 1964). Our measurement agrees with that of Fisher *et al.* (*4*), who found that Cyg XR-1 is about 5 times weaker than the measurement of Bowyer *et al.* and also that the radiation is harder than that from Sco XR-1. The data of Fig. 7 may be fitted with a straight line such that $I(h\nu) \propto (h\nu)^{-0.5\pm0.2}$.

Our measured source intensities between 1 and 20 kev are: Sco XR-1 is equal to 5.5×10^{-7} erg/(cm^{-2} sec^{-1}); Tau XR-1 is equal to 8×10^{-8} erg/(cm^{-2} sec^{-1}); Cyg XR-1 is approximately 2×10^{-8} erg/(cm^{-2} sec^{-1}). The spectra of these three sources are obviously different. This study does not eliminate synchrotron radiation as a possible source mechanism for Sco XR-1. Since the spectrum expected from a synchrotron radiation source is dependent on the electron-energy spectrum and magnetic field strength, the measured spectrum from the Scorpius source can be attributed to synchrotron radiation if one assumes an electron energy spectrum different from that assumed for the Crab Nebula.

Note added in proof. A recent measurement (*11*) has also shown that the intensity of Cyg XR-1 has greatly decreased. This experiment also resolved several sources in the Cygnus region. Accordingly, the spectrum given in Fig. 7 probably contains x-rays from both Cyg XR-1 and the radio galaxy Cyg-A.

R. J. GRADER, R. W. HILL
F. D. SEWARD, A. TOOR
Lawrence Radiation Laboratory, University of California, Livermore

References and Notes

1. R. Giacconi, H. Gursky, F. R. Paolini, B. Rossi, *Phys. Rev. Letters* **9**, 439 (1962).
2. S. Bowyer, E. T. Byram, T. A. Chubb, H. Friedman, *Science* **146**, 912 (1964).
3. ———, *ibid.* **147**, 394 (1965).
4. P. C. Fisher, H. M. Johnson, W. C. Jordan, A. J. Meyerott, L. W. Acton, *Astrophys. J.* **143**, 203 (1966).
5. G. Chodil *et al.*, *Phys. Rev. Letters* **15**, 605 (1965).
6. L. E. Peterson, A. S. Jacobson, R. M. Pelling, *ibid.* **16**, 142 (1966).
7. R. Giacconi, H. Gursky, J. R. Waters, *Nature* **207**, 572 (1965).
8. A. G. W. Cameron, *ibid.* **205**, 787 (1965).
9. B. Rossi, *Space Research* (North-Holland, Amsterdam, 1965), vol. 5, p. 1.
10. P. Morrison, *Encyclopedia of Physics* (Springer-Verlag), vol. 46, No. 1, p. 36.
11. E. T. Byram, T. A. Chubb, H. Friedman, unpublished data.
12. We thank personnel of the U.S. Naval Missile Center and the Pacific Missile Range, Point Mugu; and of U.S.S. *Wheeling* for their smooth handling of the rocket system and the launch arrangements. C. Cornell, J. Harri, J. Ronchetto, R. Rumble, and D. Salmi of Lawrence Radiation Laboratory provided technical assistance. Work performed under the auspices of AEC.

23 March 1966

Copper Artifacts: Correlation with Source Types of Copper Ores

Abstract. *Six out of eight minor chemical elements, determined by spectroscopic and neutron-activation techniques, were found to be critical in computing a probability that a given copper artifact was derived from one of three types of copper ore: native metal, oxidized ore, reduced ore. Two elements, gold and tin, were apparently alloyed deliberately in many artifacts from both the Old World and the New World.*

Copper, one of the earliest known metals, has played a very important role in the history of man. One of the intriguing problems associated with it has been the identification of the types of ores and the location of the mining areas used by ancient civilizations. If the relationship between artifacts and copper source could be established, a clearer picture of trade and travel between different areas could be obtained. Several studies along this line have been undertaken in the past (*1*). The earlier investigators surveyed impurities present in various ores and sought to associate them with impurities present in artifacts on the assumption that they would alloy in significant amounts in the copper formed. This is, of course, not necessarily the case. Most of the analyses were based on conventional chemical or spectrographic techniques. In the work we now describe various ore types and artifacts were analyzed by optical spectrographic methods of high sensitivity and by neutron activation. The latter method was employed for those metallic impurities which were below the limits of spectrographic detection. Activation techniques are very useful in the study of impurities in native copper since the metal, as it occurs naturally, is essentially spectroscopically pure.

In addition to analyzing ore minerals, metallic copper was produced from them by chemical reduction in what was considered to be the simplest, most primitive method possible. Each ore was ground with charcoal and the mixture was heated in a crucible to about 1300°C; the metal formed